Proceedings of the 17th International Conference on Nuclear Engineering
ICONE17
July 12-16, 2009, Brussels, Belgium

ICONE17-75008

DEVELOPMENT OF A NEW SPACER GRID FORM TO ENHANCE THE INTEGRITY OF FUEL ROD SUPPORT AND THE CRUSH STRENGTH OF A SPACER GRID ASSEMBLY

Kee-nam Song
Korea Atomic Energy Research Institute(KAERI)
P.O.BOX 105 Yusong, Daejon, KOREA
Phone:82-42-868-2254, Fax: 82-42-863-0565
knsong@kaeri.re.kr

Soo-bum Lee
Univ. of Maryland

Moon-Kyun Shin
Hanyang Univ., Ansan, 425791
Phone:82-31-400-4065, Fax: 82-31-408-6190

Jae-Jun Lee
Hanyang Univ., Ansan
Phone:82-31-400-4065

Gyung-Jin Park
Hanyang Univ., Ansan
Phone:82-31-400-4065

Keywords: Spacer Grid, Nuclear Fuel Assembly, Impact Strength, Dimple, Optimization

ABSTRACT

A spacer grid is one of the most important structural components in a LWR fuel assembly. The spacer grid, which supports nuclear fuel rods laterally and vertically with a friction grip, is an interconnected array of slotted grid straps welded at the intersections to form an egg-crate structure. Dimples and springs are stamped into each grid strap to support the fuel rods. The form of grid straps and spring form is known to be closely related with the crush strength of spacer grid assembly and the integrity of fuel rod support, respectively. Zircaloy is prevailing as the material of the spacer grid because of its low neutron absorption characteristic and its successful extensive in-reactor use. The primary considerations are to provide a Zircaloy spacer grid with crush strength sufficient to resist design basis loads especially due to seismic accidents, without significantly increasing pressure drop across the reactor core. Generally, the thickness and height of the Zircaloy grid strap have been the main design variables in order to meet the above considerations. Recently, it was reported that a dimple location is also a design variable that affects the crush strength of a spacer grid assembly. In this study, a new spacer grid form was developed in order to enhance the integrity of the fuel rod support and the crush strength of the spacer grid assembly by using a systematic optimization technique. Finite element analysis and crush strength tests on the developed new spacer grid form were carried out to check the performance enhancement compared to commercial spacer grids. The enhancement of fuel rod support was confirmed by comparisons of contact area, peak stresses, plastic deformation and etc. According to the results, it is estimated that the actual critical load enhancement of the spacer grid assembly is approximately up to 30 % and the actual contact area, when a fuel rod inserted into a spacer grid cell, is more than double for the developed new spacer grid form. And also, some design variables that effect the crush strength of a PWR spacer grid assembly were classified and their effects on the crush strength were investigated by a finite element analysis and a crush strength test.

1. INTRODUCTION

A fuel assembly in a Pressurized light Water Reactor (PWR) consists of spacer grids, fuel rods, a top nozzle, one bottom nozzle, guide tubes, and an instrumentation tube as shown in Fig. 1. Among them the spacer grid assembly is an interconnected array of slotted grid straps, welded at the intersections to form an egg crate structure. The spacer grid assembly supports the fuel rod with springs and dimples within a spacer grid cell as shown in Fig. 2. And also the

spacer grid protects the fuel rods from external impact loads in an abnormal operating environment such as an earthquake or a Loss-Of-Coolant Accident (LOCA). Moreover, the spacer grid assembly must maintain the instrumentation tube straight so that a plant's neutronic instrumentation can be inserted freely and removed from the tube even after the lateral loading conditions have been exceeded. Therefore, plastic deformation of a spacer grid assembly needs to be designed to have enough impact lateral strength [1].

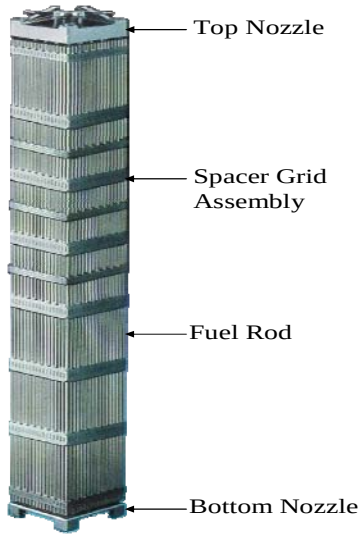

Fig. 1 PWR fuel assembly

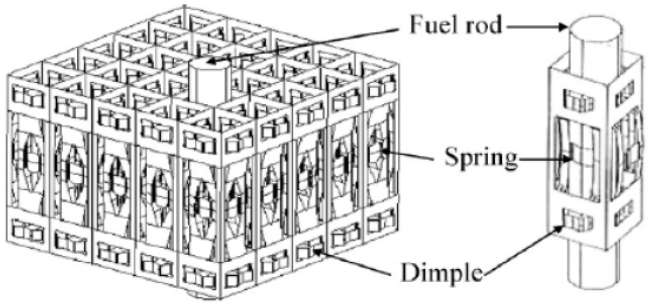

a) Spacer grid and unit cell

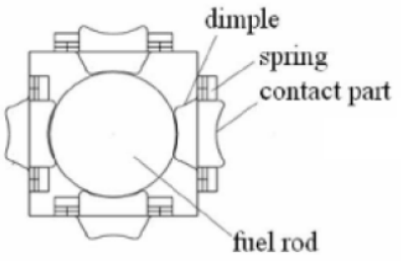

b) Cross-section of unit cell

Fig. 2 Spacer grid and cross-section of spacer grid unit cell

Several studies have been devoted to the experiments, analyses and design of a spacer grid [2-7]. The design and material for a spacer grid and design optimization of the outer plate in a spacer grid has been performed by considering the stiffness, impact strength, and the flow restriction [2, 3]. The buckling behavior is one of the important performances to evaluate the lateral strength because the deformation of spacers needs to be limited to safely maintain the guide thimbles in an abnormal operating condition such as an earthquake [4, 5]. A finite element (FE) method for predicting the buckling behavior of a spacer grid structure has been established, reflecting a real test environment, by a commercial finite element (FE) code ABAQUS/Explicit [6-8]. An effort to improve the buckling resistance of a support grid using an axiomatic design and optimization skills has been reported [9, 10], where the dimple location and the welding penetration depth at the intersection of the grid was been studied and optimized.

2. EHANCEMENT of a FUEL ROD SUPPORT

Mostly, structural design is performed in order to maximize a structural performance while constraints are satisfied. The constraints are usually imposed on the deformations or stresses, etc. In some problems, we may have a constraint to maintain a specific geometric shape of a structure. Such constraints exist in the designs of the satellite antenna, the main reflector of a large telescope, the truss structure which must maintain a certain geometric shape like a quadratic equation, the smart structure which generates a specific response values, etc. [11, 12].

Homology Design

The homology deformation defined by Hoerner [13] is to be maintained to have a certain geometric shape of a structure with a given number of structural points before, during, and after the deformation. Homology design is a design method which holds a given geometrical shape based on the homology deformation. In order words, designers predict the deformation or the natural frequency of the entire structure or a part. In homology design, design variables are determined to have the predicted response values [2, 12, 14]. In the optimization of the spacer grid spring, homology deformation, which holds a certain shape after deformation is utilized.

Condition to enhance the fuel rod support

It is well known that the shape of the spring has a great influence on the fuel rod fretting wear from experiments [2, 15, 16]. In order to minimize the fretting wear, design of the spacer grid should be performed to have a large contact area between the spring and the fuel rod [17]. From the viewpoint of homology design, the deformed shape of the spring should be the same as that of the fuel rod. If the contact area is larger, the surface pressure will be reduced, and the fretting wear will be reduced.

Two conditions for reducing the fretting wear are proposed. First, the fuel rod and the spring should have the same curvature in the section of the fuel rod. Thus, the design is formulated to minimize the difference between the two curvatures. Second, the shape of the spring center should be straight in the direction of the fuel rod. These conditions are imposed as constraints of the optimization process.

Formulation for Optimization

In order to enhance the resistance of fretting wear and the stable support of the fuel rod, the contact area between a spacer grid spring and a fuel rod should be enlarged when the fuel rod inserted in the spacer grid cell and this condition means that the deformed shape of the spring should be the same as that of the fuel rod. The deformation of the fuel rod is negligible; therefore, the fuel rod is assumed to be rigid. This condition is defined as a homology constraint and used in the optimization process.

The objective function is defined by using the homology conditions. The shape of the spacer grid spring is presented in Fig. 3. Homology constraints are defined on the x-y plane and the y-z plane in Fig. 3. The objective function is defined with several nodes because the objective function cannot be defined with all the nodes of the contact area in the spring. The objective function on the x-y plane is the minimized difference between the curvatures of the fuel rod and the deformed spring.

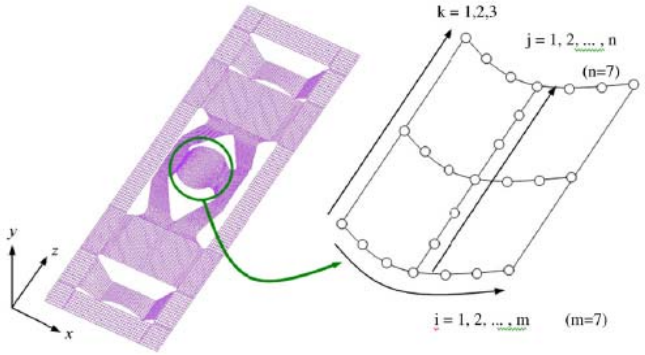

Fig. 3 Choice of nodes for homology constraint

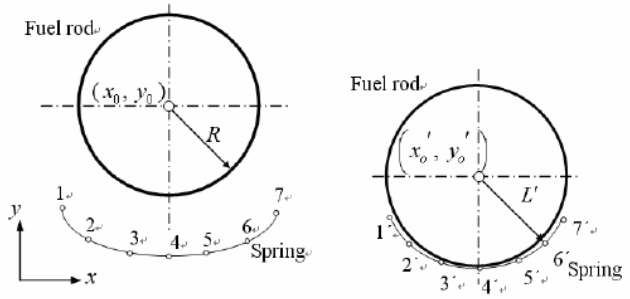

(a) Before deformation (b) After deformation

Fig. 4 Contact between the spring and the fuel rod (radial)

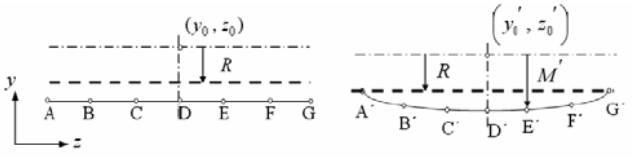

(a) Before deformation (b) After deformation

Fig. 5 Contact between the spring and the fuel rod (axial)

As illustrated in Fig. 4, seven nodes are selected for the objective function on the x-y plane. The objective function on the x-y plane is as follows:

$$\sum_{j=1}^{7}\left(R-L_j^{'}\right)^2 \tag{1}$$

where R is the radius of the fuel rod, $L^{'}$ is the distance from the selected nodes of the spring to the center of the fuel rod after deformation. Three nodes are selected on the z direction in the same way. The objective function in the z direction is as follows:

$$\sum_{k=1}^{3}\sum_{i=1}^{7}\left(R-L_{ik}^{\prime}\right)^2 \tag{2}$$

The objective function on the y-z plane is that the deformed shape of the spring center should be straight. As illustrated in Fig. 5, seven nodes are selected for the objective function. This objective function is as follows:

$$\sum_{j=1}^{7}\left(R-M_j^{\prime}\right)^2 \tag{3}$$

where $M^{'}$ is the distance from the deformed spring center to the selected nodes. The difference between $M^{'}$ and the radius of the fuel rod should be minimized in Eq. (3).

The final objective function used for optimization is a multi-objective function of each plane by the weighting factor. This objective function is as follows:

$$(1-\alpha)\sum_{k=1}^{3}\sum_{i=1}^{7}\left(R-L_{ik}^{\prime}\right)^2+\sum_{i=1}^{7}\left(R-M_j^{\prime}\right)^2 \tag{4}$$

Equation (4) is a homology equation. Constraints for optimization are defined. First, the weight of the spacer grid (w) should not be larger than that of the initial model ($w_{initial}$). Second, due to the radiation by neutron in the reactor, only 8% of the initial spring force remains after long-term operation. A load about 2 N from the fluid-induced vibration and a load about 1.2 N from the transport of nuclear fuel assembly are applied to the spring. Therefore, the initial spring force must be greater than 40 N to support the fuel rod throughout the operating period [18]. As mentioned earlier, the spring force is the reaction force at the edges of the spacer grid. Third, the height of the spring center is (h_c) before deformation must be larger than 1.65 mm. This is shown Fig. 6. If the height of the spring center is smaller than 1.65 mm, the spring force is smaller than 40 N in non-linear static analysis after optimization. It is formed from numerical experiment. Finally, the stress of spacer grid (σ) is smaller than the allowable stress of the spacer grid ($\sigma_{allowable}$).

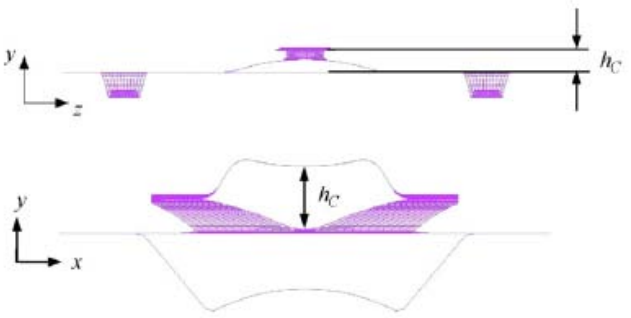

Fig. 6 Height of spring center

$$
\begin{aligned}
&\text{Find} && b_n \quad n = 1, \cdots, 29 \\
&\text{to minimize} && (1-\alpha)\sum_{k=1}^{3}\sum_{i=1}^{7}(R - L'_{ik})^2 + \sum_{j=1}^{7}(R - M'_j)^2 \\
&\text{subject to} && w \le w_{\text{initial}} \\
& && F_{\text{spring}} \ge 40\,\text{N} \\
& && h_C \ge 1.65\,\text{mm} \\
& && \sigma \le \sigma_{\text{allowable}}
\end{aligned}
\qquad (5)
$$

Equation (5) is the formulation for optimization. However, this formulation cannot include the plastic deformation. Therefore, it is necessary to convert the formulation so as to permit the plastic deformation and to reduce the maximum stress. This formulation is converted to a min-max problem. When a maximum property is included in the optimization formulation, the problem can be solved by using the Taylor-Benson 'beta' formulation as follows:

$$
\begin{aligned}
&\text{Find} && b_n && n = 1, \cdots, 29 \\
&\text{to minimize} && \beta \\
&\text{subject to} && w \le w_{\text{initial}} \\
& && F_{\text{spring}} \ge 40\text{N} \\
& && h_C \ge 1.65\text{mm} \\
& && \left(R - L'_{ik}\right)^2 \le C_h && i = 1, \cdots, 7; k = 1, 2, 3 \\
& && \left(R - M'_j\right)^2 \le C_h && j = 1, \cdots, 7 \\
& && \sigma \le \beta
\end{aligned}
\qquad (6)
$$

where β is the artificial variable used for the objective function of a min-max problem, new constraints (C_h) are defined on each plane. Thus, the artificial variable β is minimized while the constraints including all the stresses are satisfied. It is noted that Eq. (6) does not have a constraint for allowable stress so that plastic deformation is allowed. The homology constraints, which must be smaller than a homology constant (C_h), are defined on each plane. The homology constant should be appropriately defined.

Flow Chart for Optimization

A design process is defined as illustrated in Fig. 7. It is extremely difficult to directly consider non-linear analysis in structural optimization. It is desirable to exploit the benefit of linear static optimization. First, linear response optimization is performed with the initial model. To verify the optimization process, non-linear static analysis is performed with the optimized model. If the analysis results satisfy the convergence criteria, the optimization process is terminated. Otherwise, as mentioned earlier, new loads are calculated with the results of non-linear static analysis and optimization is performed again by using the new loads until the convergence criterion is satisfied. The convergence criterion is defined by the total distance which is the sum of the distances between all the nodes of the fuel rod and that of the contact part of the spacer grid spring. The distances are illustrated in Fig. 8, and the total is calculated as

$$D^j = \sum_{i=1}^{n} d_i \qquad (7)$$

If the total distance of current cycle is larger than that of the previous cycle, the optimization process is terminated. GENESIS 7.5 [19] is used for optimization of the spacer grid spring and the modified method of feasible direction (MMFD) algorithm is utilized.

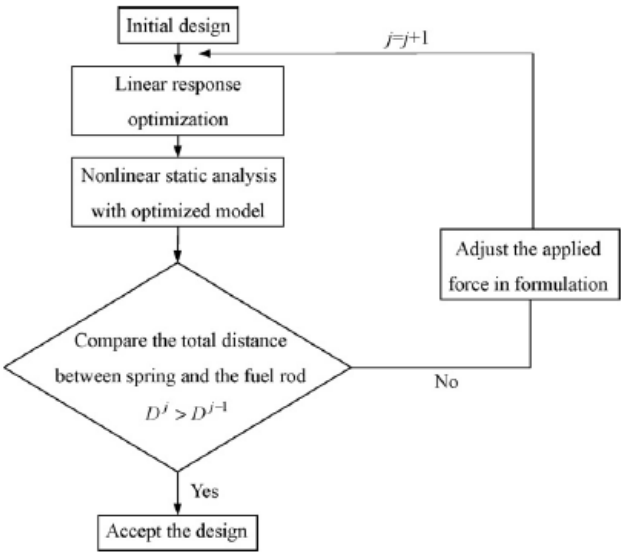

Fig. 7 Flow chart of optimization for a spacer grid spring

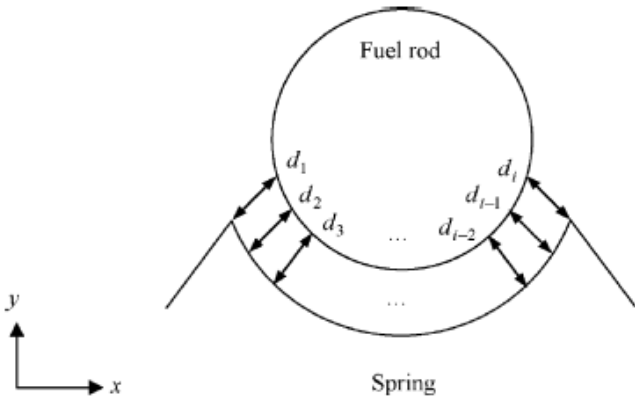

Fig. 8 The definition of the total distance

Results of Enhancement

The enhancement of a fuel rod support was confirmed by

comparisons of the contact area, peak stresses, and plastic deformation of a spacer grid spring when inserting a fuel rod into a spacer grid structure. The normalized enhancement of a fuel rod support is shown in Table 1. According to Table 1, a considerable enhancement of a fuel rod support is achieved by a design optimization using homology constraints.

Table 1 Normalized enhancement of a fuel rod support before and after optimization

Performance parameters	Before optimization	After optimization
Contact area	1.000	2.069
Peak stress	1.000	0.955
Plastic deformation	1.000	<0.333

3. EHANCEMENT of the CRUSH STRENGTH of a SPACER GRID ASSEMBLY

Strap Thickness

A grid strap's thickness has generally been considered as one of the main design variables in order to regulate the crush strength. Figure 9 shows the relations between a grid strap's thickness and crush strength, where the crush strength has a cubic relationship with a grid strap's thickness. However, this design variable for a spacer grid assembly is very closely related with the pressure drop of a coolant, its application to a spacer grid design is significantly restrictive. Therefore, we did not consider this to be an effective measure for enhancing the crush strength of a spacer grid assembly.

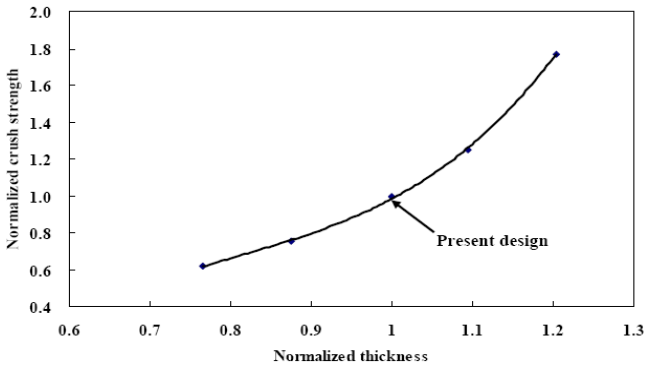

Fig. 9 Crush strength vs. strap thickness

Strap Height

A total grid strap's height has generally been considered as one of the main design variables in order to regulate a crush strength. However, this design variable for a spacer grid assembly is also very closely related with the pressure drop of a coolant, its application to a spacer grid design is significantly restrictive. Therefore, we did not consider this to be an effective measure for enhancing the crush strength of a spacer grid assembly.

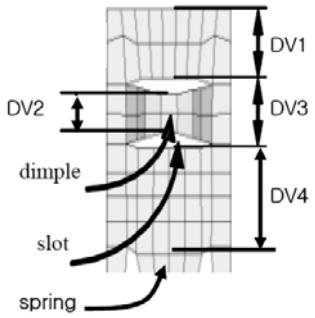

Fig. 10 Design variables for optimization of dimple location

Optimization of Dimple Location

Recently, it was reported that a dimple location is also a design variable that effects the crush strength of a spacer grid assembly. An effort to improve the crush strength of a spacer grid using an axiomatic design and optimization skills has been reported [7]. And the effect of dimple location in a spacer grid on crush strength has been investigated by parametric study of the design variables in a spacer grid strap [8]. Figure 10 shows the design variables for an optimization of a dimple location, where the spring length and the total height of a grid strap maintain constant values. So, it could be very helpful for designing a spacer grid assembly, if a new design variable is deduced without affecting the pressure drop of a coolant, so much. Therefore, we did consider this to be an effective measure for enhancing the crush strength of a spacer grid assembly.

Increase the Weld Line Length

The crush strength of a spacer grid assembly is strongly related to the buckling strength of the spacer grid straps constituting the spacer grid assembly. Based on the fact that the critical load (P_{cr}) is proportional to the moment of inertia (I), P_{cr} can be enlarged by increasing the plate thickness (t) and the effective height (B_e) of a strap as shown in Fig. 11 and Eq. 8. B_e refers to the part in a strap where a load passes, which is smaller than the height of a strap (B_1+G+B_2).

$$p_{cr} \propto \frac{EI}{L^2} \propto B_e \bullet t^3 \qquad (4)$$

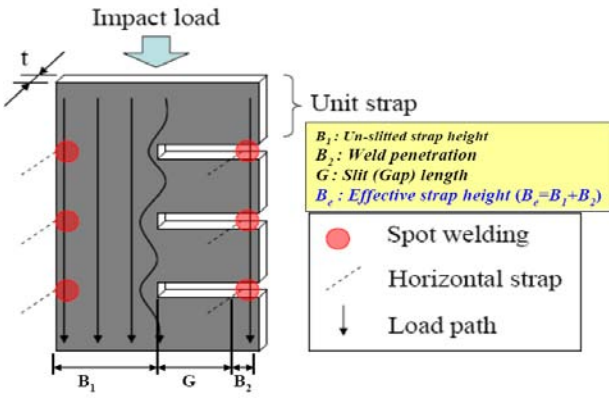

Fig. 11 Effective height for a grid strap

Fig. 11 shows a simple case where there are no dimples and springs, and we can improve P_{cr} by increasing B_e or reducing the slit (gap) length (G). Therefore, increasing the effective height including the weld line length by maintaining the total height of the grid straps, could increase the bucking strength of the grid straps, consequently, also the crush strength of the spacer grid assembly without increasing the pressure drop of a coolant.

Nowadays, laser beam welding (LBW) is prevailing for most of the Zircaloy spacer grid manufacturing vendors, for the purpose of a smaller bead size and a larger weld penetration at the welding parts. A spacer grid assembly with a smaller bead size leads to a smaller pressure drop of the coolant flowing along the fuel assembly, which consequently leads to a reduction in the load on a reactor coolant pump. In addition, a spacer grid assembly with a deeper weld penetration results in a larger crush strength of a spacer grid assembly, which is very important for the seismic resistance of a nuclear fuel assembly. However, a conventional laser spot welding with a high energy input at the intersection points usually results in spattering and larger bead size, which is a demerit for a spacer grid assembly performance in reactors. Hence, a seam welding method along an intersection between inner grid straps could be proposed as one of the alternatives to solve these demerits. We developed a new welding technique and a welding unit in the case of using the same LASER welder (Miyachi ML-2550A) of for a conventional spot welding. The new LBW technique is constructed by tilting the LASER beam along the intersection line of the spacer grid assembly in order to obtain a longer weld line and a smaller weld bead size. Tilting the LASER beam is achieved by using the apparatus as shown in Fig. 12 [20]. Weld lines for the new LASER welding technique are illustrated in Fig. 13 in the case of a continuous seam weld and an intermittent seam weld, respectively.

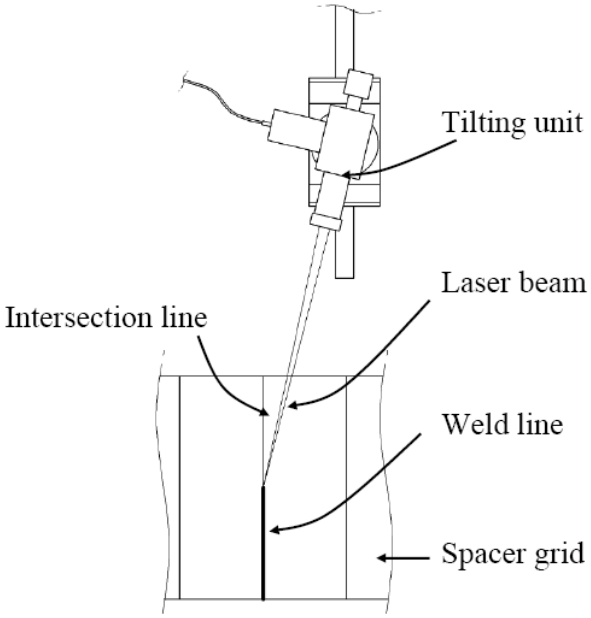

Fig. 12 Proposed LASER welding techniques (Tilting unit)

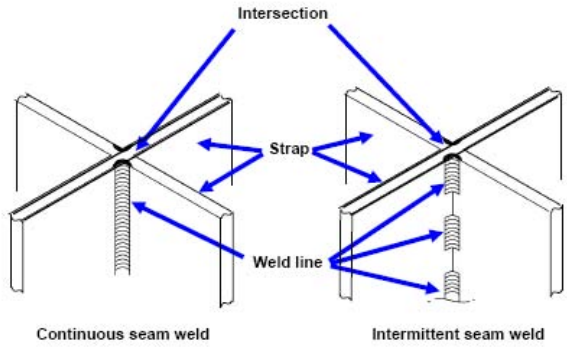

Fig. 13 Weld line for the proposed LASER welding techniques

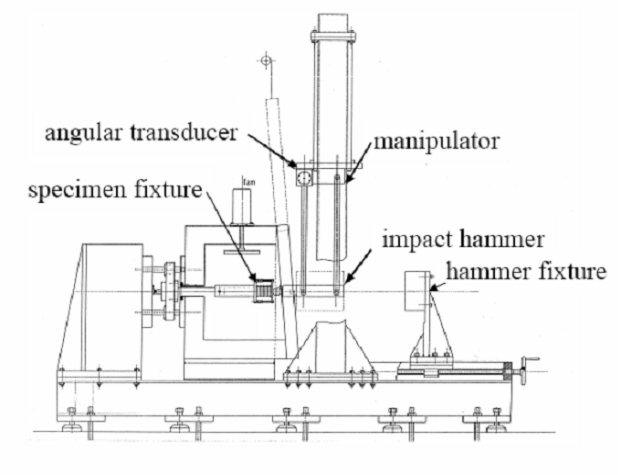

Fig. 14 Crush strength tester

4. CRUSH STRENGTH ANALYSIS AND TEST

Crush strength test

A pendulum type impact tester as shown in Fig. 14 was used to perform the impact test of the spacer grid assembly. It is intended to simulate the type of load and impact velocities anticipated under a seismic disturbance. This tester is composed of a structural body, an impact hammer, a data acquisition system and a furnace. The impact hammer is composed of a sphere type impact tip for a dynamic loading and two sensors, which are two force transducers and one accelerometer, for gathering the dynamic data. An angular transducer is attached at the hinge point of the impact hammer in order to detect the initial angle of the hammer and to obtain continuous data on the angle of it. The data acquisition system consists of a magnetic controller, two dynamic signal amplifiers, and a temperature controller. The impact hammer moves with the guidance of the four guide rods. The impact hammer is made of a mild steel, which mass corresponds to the mass of one span of the spacer grid assembly. The manipulator at the hinge point of the impact hammer is made for an accurate impact point regardless of a specimen's size. The general test setup consists of the floor, hammer weight, force transducer, dynamic accelerometer, and mounting fixtures. The specimen is fixed to the holding fixture by two screws. The impact hammer is held by a

magnetic holder and released when a release signal on the controller is activated.

FE Analysis

First of all, the FE modeling of the 3×3 spacer grid assembly has been done by interconnecting the slotted grid straps and welding the intersections as shown in Fig. 15. The intersecting part is simply illustrated in Fig. 15(a), where the position of a spot welding is indicated as circles at both ends. In the FE model, six node solid elements are used to model the welding bead which shares the nodes with the shell elements, and contact conditions are applied along the intersecting slots (the enlarged subfigures in Fig. 15(b)); the two intersecting straps at 90 degrees do not interfere with each other. In this FE model, S3R (3-node triangular general-purpose shell, finite membrane strains), S4R (4-node doubly curved general-purpose shell, reduced integration with hourglass control, finite membrane strains) shell elements and C3D6 (6-node linear triangular prism) solid elements in ABAQUS [21] have been used: a total of 7246 nodes and 6070 elements.

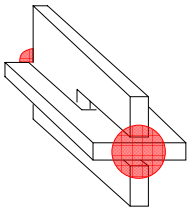

(a) Simplified view

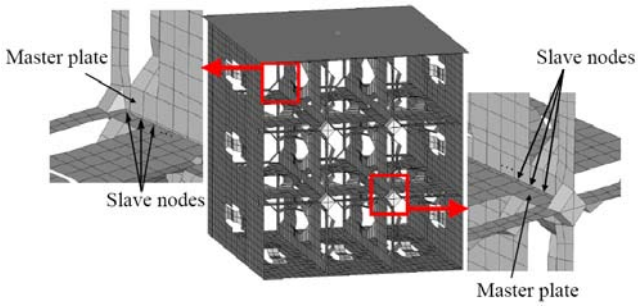

(b) Enlarged view

Fig. 15 Detailed view at an intersection

The FE analysis is carried out by considering a real impact experiment environment as follows. 1) An impact hammer is modeled as a rigid element with an equivalent mass. 2) The contact condition is applied between the rigid plate and the support grids. 3) The nodes at the bottom plate are fixed. The FE analysis model is shown in Fig. 16. The initial impact velocity at the reference node (at the center of the upper rigid surface) is applied, and the output accelerations for the initial impact velocity are obtained at this node. The impact force of the grid is evaluated: by multiplying the maximum acceleration of the model by the mass of the impact hammer. The impact analyses are done for different velocities from 381 mm/s and by an increasing increment of 63.5 mm/s. The impact force generally increases as the velocity increases, but for a certain case it decreases where the structure is considered to experience buckling. The critical impact load (crush strength) is taken as the impact force from this case where the peak point is observed.

Second, the FE models for the sub-sized (7x7 type) and the fully arrayed (16x16 type) spacer grid assembly for the impact analysis were also modeled. Figures 17 and 18 show the FE models for the sub-sized and the fully arrayed spacer grid assembly, respectively. In the FE analysis model, a rigid and mass element were used for the impact hammer as shown in Figs. 17 and 18. All degrees of freedom were fixed at the rigid surface of the bottom side as shown in Figs. 17 and 18.

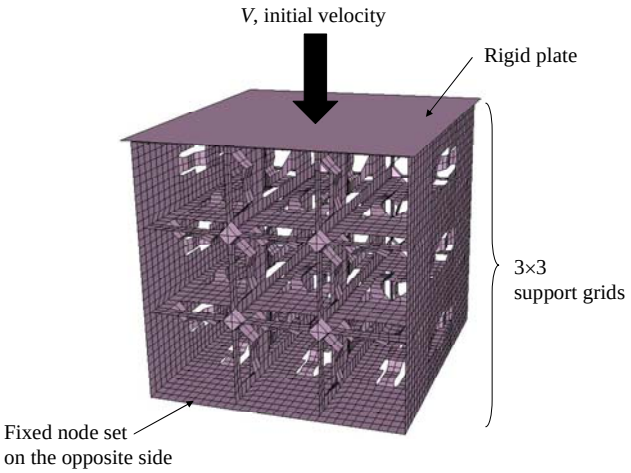

Fig. 16 Load and boundary conditions

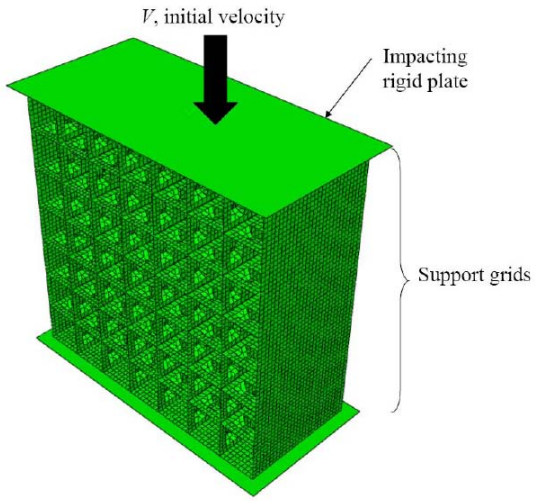

Fig. 17 Boundary and loading conditions for the sub-sized spacer grid assembly

It is known that a welding penetration depth affects the crush strength of a spacer grid assembly to some extent [7]. Crush test and FE analysis for the sub-sized (7x7 type) spacer grid assembly shown in Fig. 17 were performed. Table 2 shows the geometric data for the sub-sized specimen and Table 3 shows the test and analysis results for the sub-sized specimen. The test results were obtained from an average of 5 or 13 specimens. According to Table 2, the tendencies of a

crush strength increase from the analysis are in good agreement with those from the test. The discrepancy between the test and the analysis results is attributed to the manufacturing dimensional tolerances and a local thinning of the strap thickness around the welded parts, whereas fixed dimensions were assumed in the analysis. We found that the crush strength was enhanced by up to 34 % with an increase of the weld line when compared with that of the conventional spot welding method for the 7x7 sub-sized spacer grid specimen.

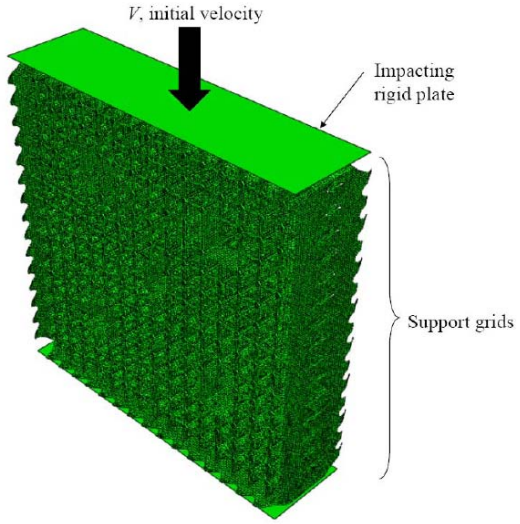

Fig. 18 Boundary and loading conditions for the full-arrayed spacer grid assembly

Figure 19 shows the normalized crush strength enhancement for the fully arrayed spacer grid assembly with guide tubes from the test and FE analysis with an increase of the normalized weld line length. The crush strength enhancement has a good linear relation with the weld line length as shown in Fig. 19 from the finite element analysis and test. According to Fig. 19, a considerable crush strength enhancement, i.e. up to 60%, was achieved by the proposed welding method compared to that by the conventional spot welding method

Table 2 Geometric data for the sub-sized specimens

Specimen (7x7 type)	Strap thickness (mm)	
	Outer strap	Inner strap
	0.664	0.457

Table 3 Buckling strength increase ratio based on the value of a welding point at an intersection for the sub-sized specimen

Weld penetration (mm)	Analysis	Test	Remark
Point welding (2.0)	1.000	1.000	Conventional weld
9.275	1.145	1.154	
13.280	1.337	1.373	

5. CONCLUSIONS

New spacer grid form was developed in order to enhance the integrity of a fuel rod support and the crush strength of a spacer grid assembly by using a systematic optimization technique. The enhancement of the fuel rod support was confirmed by comparisons of the contact area, peak stresses, and plastic deformation etc. while the enhancement of the crush strength was investigated for a 3x3 and 7x7 sub-size support grid as a preliminary parameter study for a 16x16 full size support grid. And the enhancement of the crush strength due to the increase of the weld line length was also investigated for a spacer grid assembly with the guide tubes from the test and FE analysis.

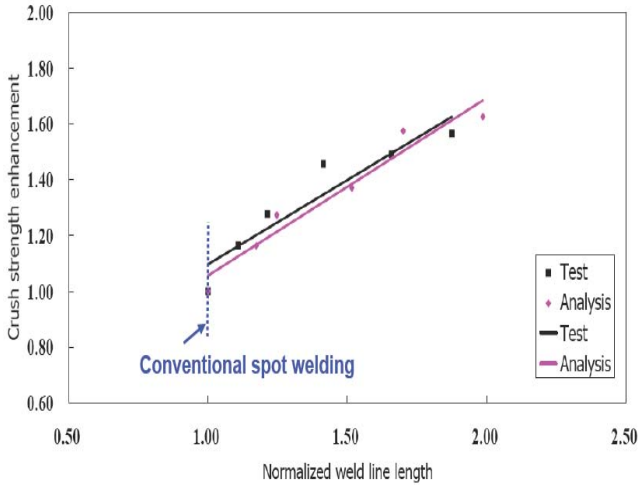

Fig. 19 Crush strength enhancement for the fully arrayed spacer grid assembly with guide tubes

Acknowledgments

This work described in this paper was supported by the SMBA (Small and Medium Business Administration of Korea).

References

(1) H.J. Kunz, R. Schiffer, K.N. Song, "Fuel assembly mechanical design manual," Siemens/KWU Work-Report U6 312/87/e326 (1987).

(2) L.A. Walton, "Zircaloy spacer grid design," Trans. Am. Nucl. Soc., 32, 601-602 (1979).

(3) J.G. Larson, "Optimization of the Zircaloy space grid design," Trans. Am. Nucl. Soc., 43, 160-161 (1982).

(4) K.H. Yoon et al., "Shape optimization of the H-shape spacer grid spring structure," J. Korean Nucl. Soc.(Nuclear Engineering and Technology), 33, 5, 547-555 (2001).

(5) K.N. Song et al., "Shape optimization of a nuclear fuel rod support structure," 16th Int. Conf. on Structural Mechanics in Reactor Technology, Washington, DC, U.S.A., Aug. 12-17 (2001).

(6) K.H. Yoon et al., "Dynamic impact analysis of the grid structure using multi-point constraint (MPC) equation under the lateral impact load," Computers & Structures, 82(23-26), 2221-2228 (2004).

(7) S.H. Lee et al., "Design improvement of an OPT-H type nuclear fuel rod support grid by using an axiomatic design and an optimization," Journal of Mechanical Science and Technology, 21, 1191-1195 (2007).

(8) S.B. Lee et al., "Parametric study of a dimple location in a spacer grid under a critical impact load," Journal of Mechanical Science and Technology, 22, 2024-2029 (2008).
(9) J.K. Kim, "Shape optimization of a nuclear fuel rod spacer grid considering impact and wear," Master thesis, Hanyang University, Korea (2007).
(10) M.K. Shin et al., "Optimization of a nuclear fuel spacer grid spring using homology constraints," ICONE 15-10366 (2007).
(11) K.H. Lee et al., "Truss optimization considering homologous deformation under multiple loadings," Structural Optimization, 16(2-3), 193-200 (1998).
(12) K.H. Lee and G.J. Park, "Structural homology design using equality constraints," Proc. of the Sixth Int. Con. on Adaptive Structures, Miami, FL, USA (1995).
(13) S.V. Hoerner., "Homologous deformation of tilttable telescopes," J. Struct. Div. , Proc. ACSE93, 461-485 (1967).
(14) Nakagiri, S. et al., "A note on finite element synthesis of structures," part 7, Formulation of homologous vibration mode, 44, SEISANKENKYU, Institute of Industrial Science, Univ. of Tokyo, No. 9, 449-452 (1992).
(15) J.W. Ha et al., "Experimental analysis on the influences of support condition and shape in fuel fretting wear," Proc. of the Korea Nuclear Society Fall Annual Meetings, Yongpeong, Kangwondo, Korea (2002).
(16) Kennard, M.W. et al., "A study of grid-to-rod fretting wearin PWR fuel assemblies," vol.1 S.M.Stoller co., Broomfield, CO, USA (1995).
(17) Y.H. Lee et al., "Effects of contact shape and environment in fuel fretting wear," Proc. of the Korea Nuclear Society Fall Annual Meetings, Yongpeong, Kangwondo, Korea (2002).
(18) K.N. Song et al., "Design of a nuclear fuel rod support grid using axiomatic design," Trans. of Korea Society Mechanical Engineers A, 26, 8, 1623-1630 (2002).
(19) GENESIS User's manual, Version 7.5, Vanderplaats Research and Development Inc., Cplorado Springs, CO, USA (2004).
(20) K.N. Song and S.S. Kim, "Development of a LASER welding apparatus for welding along the intersection line of the inner straps for a PWR spacer grid assembly and its application," Proceedings of LPM2008, Quebeck, Canada, June (2008).
(21) ABAQUS Analysis User's Manual, Version 6.7 (2007).